Ragheed M. Ibrahim
Ivan B. Karomi

Department of Physics, College of Education for Pure Science, Mosul University, Mosul, IRAQ

Effect of Tapered Length on Operation of Traveling-Wave Semiconductor Laser Amplifier: A Numerical Study

This article presents a simulation study on the effect of varying tapered buried ridge stripes of the active region length on the performance of InP–InGaAsP semiconductor laser amplifier (SLA). The gain bandwidth, noise figure, amplified spontaneous emission, and output noise power are analyzed using a numerical wideband steady-state model for tapered lengths ranging from 25µm to150 µm. The model involves a set of traveling-wave equations that define signal fields and photon rates with the rate equation. The results show at 3-dB point, SLA revealed a wide signal wavelength range with a gain up to 26.7 dB for an active region tapered length of 50 µm. Moreover, the gain of the SLA exhibited the lowest value at a current of 120 mA with a low noise of 2.3 dB when the tapered length was 25µm. Finally, the results showed that the noise power is inversely related to the tapered length, whereas it increases with the bias current.

Keywords: Semiconductor laser; Laser amplifier; Tapered waveguide; Traveling-Wave
Received: 31 May 2024; Revised: 30 June 2024; Accepted: 07 July 2024

1. Introduction

The main technique of transmitting data information around the world is optical technology. The tremendous and rapid growth of the data traffic internet and its various service applications, requires the exchange of large amounts of data at high speed rate. This leads to the emergence of a new generation of optical networks to meet these requirements. The most promising technology for this type of optical network is using of the unique features of semiconductor laser amplifier (SLA).

The SLA, which has been distinguished from other kinds of optical amplifiers, is the most significant and promising optoelectronic device to be an essential element in most optical networks. [1] This is mostly due to their larger bandwidth, smaller size, lower cost, electrical pumping, potential to be integrated on a chip [1,2], high gain [3], low-power consumption [4], high operation rate and extremely potent non-linearity [5]. In addition, SLA works as an amplifier, its ingrained nonlinearity enables it to serve as the basis for a wide range of optical signal processing functions, since there is no need to convert an optical signal into an electric domain [1,6,7]. For example SLA can be unlisted in photonic switching [8], signal regenerators [9], wavelength converters [10], clock recovery [11], optical logic gates [12] and wavelength-division-multiplexing (WDM) [13]. The same basic component could perform serval various applications by incorporating the amplifier functionality within the semiconductor material [5]. In fact, there are two major types of semiconductor optical amplifiers (SOAs). The Fabry-Perot semiconductor optical amplifier (SOA), which is characterized by substantial reflections from the end facets subsequently the signal passes via the amplifier many times and traveling-wave semiconductor optical amplifier (SOA), in which the facets reflections are reduced to less than 10^{-5}. Thus, the signal is amplified in a one pass [14-16]. So far, a vast number of researches have been conducted on the semiconductor optical amplifier (SOA) in order to improve their characteristics [3]. For instance, the main performance attributes of semiconductor laser amplifier (SLA) have been studied in [17] for different materials of semiconductor laser amplifiers; linear, nonlinear and modulated. In [18], semiconductor laser amplifier (SLA) gate performance was examined using the dynamic model of a tapered semiconductor laser amplifier. The effect of the confinement factor on the output characteristics of a tapered traveling-wave semiconductor laser amplifier (SLA) and the input field's wavelength as well as the injected current was documented in [19]. The dependence of the operating characteristics of the semiconductor laser amplifier on the active region size and the bias current have been reported in [20].

In this framework, a numerical wideband steady-state model for active region tapered length of InP–InGaAsP semiconductor laser amplifier (SLA) is modeled to reveal the effect tapered length on the operation properties of semiconductor laser amplifier (SLA).

2. Structure and Material Model of Amplifier

The semiconductor laser amplifier (SLA) used in the simulation process is a 1550 nm InP–InGaAsP tapered buried ridge stripe. Figure (1a) illustrates a schematic cross-section of semiconductor laser amplifier (SLA), while figure (1b) shows a top view of an active region. The amplifier structure consists of an InGaAsP materials embedded central active area with thickness (d), length (Lc) and width (W). In a linear, tapering pattern, the active area's breadth shrinks, with a length (L_t) and a width of W in the central zone to zero width at either end. On the other

hand, the value of the confinement factor is higher at the center of active region and decreases as we move away from the center and it becomes zero at the edges. The taper profile could play a crucial role which can improve the coupling efficiency of the amplifier facets to a single-mode optical fiber. Furthermore, the effective facet reflectance is lowered by slant the active region away from the cleavage plane. Both ends of the device have windows buried to lower the affective facet reflectivity. The mean length L of the device, as a first approximation, is given by [21].

$$L = L_c + L_t \quad (1)$$

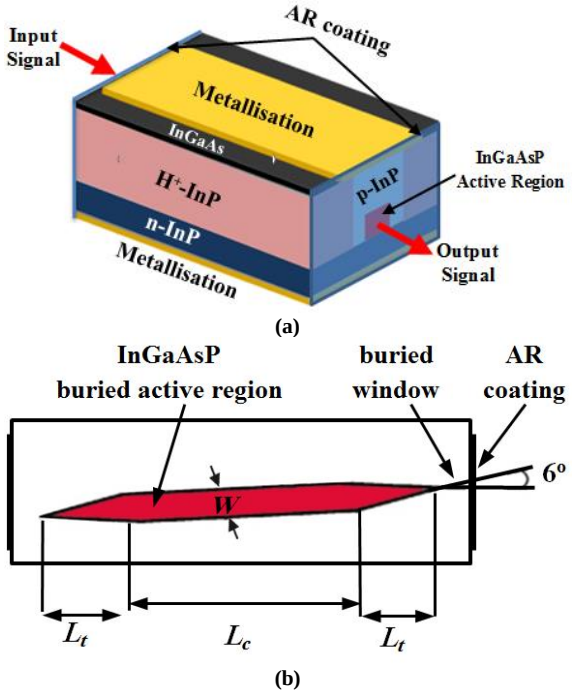

Fig. (1) Structure of the homogenous buried ridge stripe semiconductor laser amplifier (SLA) (a) cross-section (b) top view of an active region

The gain factor g_m of the InGaAsP active region is given as [22]:

$$g_m(v,n) = \left(\frac{c^2}{4\sqrt{2}\,\pi^{3/2}\,n_a^2\,\tau\,v^2}\right)\cdot\left(\frac{2m_e\,m_{hh}}{(h/2\pi)(m_e+m_{hh})}\right)^{3/2} \times\sqrt{v-\frac{E_g(n)}{h}}\,[f_c(v)-f_v(v)] \quad (2)$$

h is symbol of Planck's constant, c is light speed, τ is the radiative recombination lifetime, v optical frequency and n_a is the refractive index of active region

3. Model of Semiconductor Laser Amplifier

The travelling-wave equations defining the fields signal and rate of photons, as well as a rate equation of carrier density is used in numerical calculations to form the basis of the semiconductor laser amplifier (SLA) model. The traveling-wave equations is given as [23]:

$$\frac{dE_{S_k}^{\pm}(z)}{dz} = \left\{\mp j\beta_k \pm \frac{1}{2}\left[\Gamma g_m\left(v_k, N(z)\right) - \alpha\right]\right\} E_{S_k}^{\pm}(z) \quad (3)$$

here, $E_{S_k}^{\pm}(z)$ is a complex of wave propagation in z-directions; (β_k) is propagation factor; Γ represents the parameter of optical confinement ; $g_m(v_k , N(z))$ represents gain factor; and *(α)* is the coefficient of material loss.

The wave equations for spontaneous emission can be written as [24]:

$$\frac{dN_j^{\pm}(z)}{dz} = \pm\left[\left(\Gamma g_m\left(v_j N(z)\right) - \alpha\right)\right] N_j^{\pm}(z) + R\left(v_j N(z)\right) \quad (4)$$

where $N^{\pm}_j$ refers to the spontaneous spectrum in z-directions; and *Rsp* is the noise coupled within N^{+}_j and N^{-}_j. Therefore, carrier density at position z is determined by [24]:

$$\frac{dN(z)}{dt} = \frac{I}{edLW} - R(N(z)) - \frac{\Gamma}{dw}\left\{\sum_{k=1}^{N_s} g_m\left(v_k, N(z)\right)\left(N_{s_k}^{+}(z) + N_{s_k}^{-}(z)\right)\right\} - \frac{2\Gamma}{dw}\left\{\sum_{j=1}^{N_m-1} g_m\left(v_j N(z)\right) K_j\left(N_j^{+}(z) + N_j^{-}(z)\right)\right\} \quad (5)$$

The right-side in Eq. (5) represent; the carriers added to the active layer from the pumped current, the recombination ratio, the carriers' radiative recombination due to the amplified signal and the carriers' radiative recombination owing to spontaneous spectrum, respectively. Here, I is the amplified current, *R(N(z))* is the recombination ratio, e is electron charge, N_s is the signals inserted within semiconductor laser amplifier (SLA), $N_{s_k}^{+}$ is the photon rate, and $N_{s_k}^{-}$ is the photon rate of the electrical field in the opposite direction. according to the model proposed in [5], the noise figure (NF) can be computed numerically. The simulation parameters used in this model are presented in table (1).

3. Results and Discussion

The gain of the InP–InGaAsP semiconductor laser amplifier (SLA) against injection current at different tapered length is shown in Fig. (2) with a fixed input signal power and signal wavelength. In this simulation, different tapered length used are 25, 50, 75, 100, 125 and 150 µm with input signal power of -25dBm and signal wavelength of 1550nm, at room temperature. It is found that the amplifier gain increases when the bias current is increased before reaching saturation region. In addition, it is confirmed that the tapered lengths showed a significant impact in the gain-current relationship and this result is in agreement with [21]. Moreover, it is observed that the gain declines with increasing semiconductor laser amplifiers (SLAs) length due to the noise increase in semiconductor laser amplifiers (SLAs) [5]. Therefore, the bias current should be selected to take

high values in order to produce large gains and low noise figures. The gain variation-current curves of the sample vary when the active region tapered length is changed as it shown in Fig. (3). It is found that the gain variation decreases with increasing a driven current, and this could be because the carrier density in the active region reaches its high value.

Table (1) Values for semiconductor laser amplifier (SLA) parameters utilized in the simulation

Symbol	Definition	Value	Unit
A	Linear recombination coefficient	36×10^{7}	s^{-1}
B	Recombination factor	5.4×10^{-16}	$m^3 s^{-1}$
C	Auger factor	3.2×10^{-41}	$m^6 s^{-1}$
T	Absolute temperature	300	k
Γ	Confinement factor	0.54	-
η_{in}	Coupled-loss/ Input	4	dB
η_{out}	Coupled-loss/ Output	4	dB
R_1	Reflectivity-facet/ Input	5.5×10^{-5}	-
R_2	Reflectivity-facet/ Output	5.5×10^{-5}	-
L	Active-length	600	µm
W	Active-width	0.4	µm
d	Active-thickness	0.4	µm
v_g	Group velocity	75×10^{6}	m/s
v_τ	Transparent carrier density	1.4×10^{24}	m^{-3}
k_g	Bandgap shrinkage factor	9×10^{-11}	eVm
Eg_0	Bandgap energy	0.7825	eV
K_o	Independent-carrier for loss	6300	m^{-1}
K_1	Dependent-carrier for loss	7.6×10^{-21}	m^2
m_e	Electron effective mass	4.1×10^{-32}	kg
m_{hh}	*hh* effective mass	4.15×10^{-30}	kg
m_{lh}	*lh* effective mass	5.07×10^{-31}	kg
n_1	Active refractive index	3.22	-
dn_1	Differential of active refractive index	-1.9×10^{-26}	m^{-3}
n_{eq}	Equivalent effective refractive	3.32	-
dn_{eg}	Differential of equivalent refractive	-1.89×10^{-26}	m^{-3}

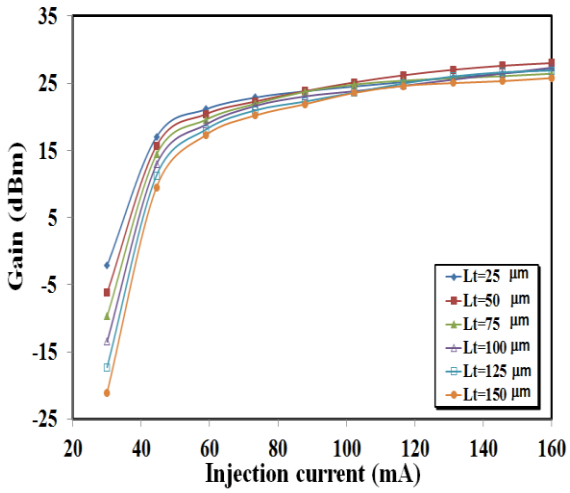

Fig. (2) Gain of semiconductor laser amplifier (SLA) against drive current, at various tapered lengths and input signal power of -25dBm, input signal wavelength of 1550nm

Figure (4) represents the simulated results of optical gain spectra for semiconductor laser amplifier (SLA) at different tapered lengths of 25, 50, 75, 100, 125 and 150µm, and injection current of 120 mA and input signal power of -25 dBm at room temperature. As the tapered length increases, the semiconductor laser amplifier (SLA) gain bandwidth gets narrower. Furthermore, the amplified spontaneous emission (ASE) spectra for semiconductor laser amplifier (SLA) at various tapered length, taken at injection current of 120 mA and constant input signal power of -25 dBm at room temperature are plotted in Fig. (5). It is evident that when the tapered length decreases the amplified spontaneous emission (ASE) increases, as a result of increases the population inversion which makes spontaneous emission more intense [25,26].

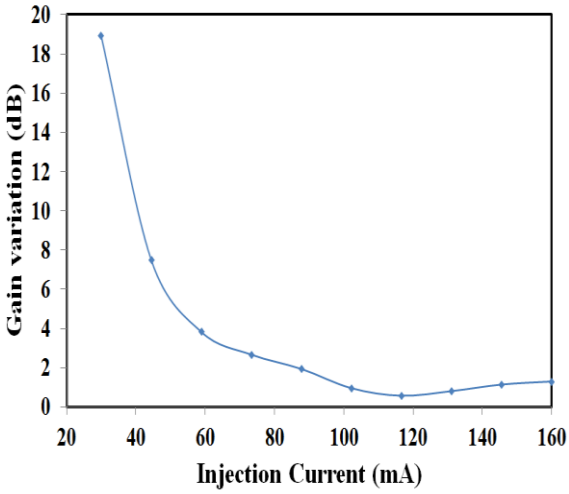

Fig. (3) The gain versus the bias current at fixed input power of -25 dBm and input signal wavelength of 1550 nm

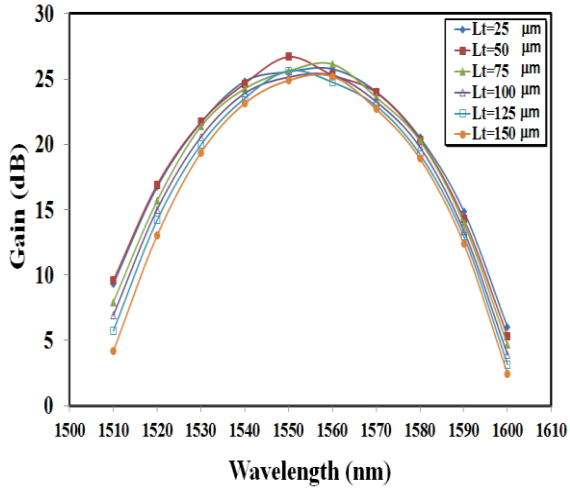

Fig. (4) Gain spectra for semiconductor laser amplifier (SLA) at different tapered lengths (25, 50, 75, 100, 125 and 150µm), injection current of 120 mA, input signal power of -25 dBm

Figure (6) displays the noise figure (NF) against the fiber-to-fiber gain at different tapered length for semiconductor laser amplifier (SLA). the noise figure (NF) trends to decrease with increasing gain and it reaches lowest value at gain of 13.3 dB (It can be

characterized as a threshold point). Consequently, an increase in gain increases the noise figure (NF) of the sample. Likewise, it is found that the noise figure (NF) fluctuated with the tapered length specially, around the threshold point.

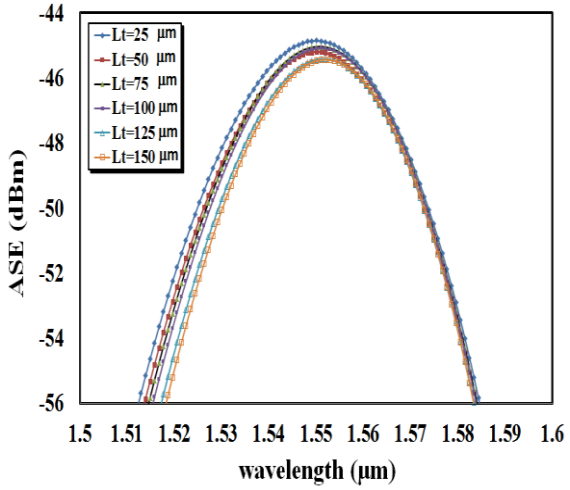

Fig. (5) Output amplified spontaneous emission (ASE) spectra at various tapered length

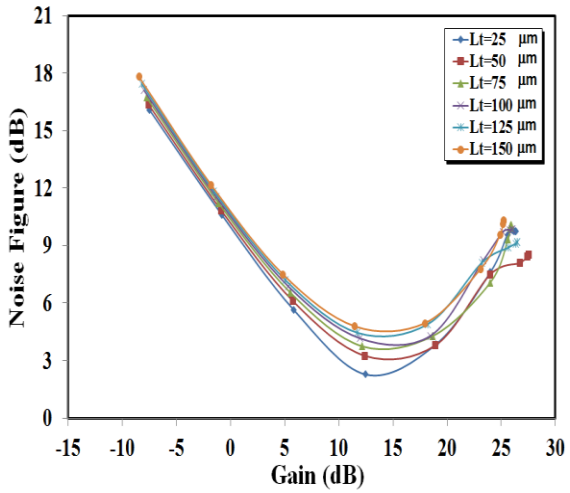

Fig. (6) Noise figure (NF) against gain for various tapered lengths

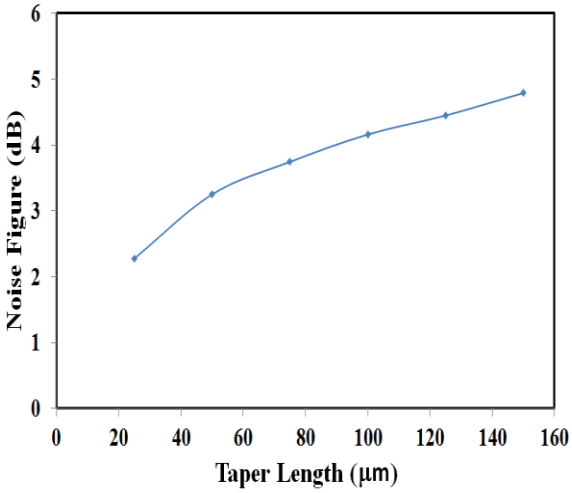

Fig. (7) Noise figure (NF) against active region tapered lengths

Figure (7) reveals data simulations of the noise figure (NF) versus tapered length at fixed; input signal power of -5 dB, drive current of 120 mA and wavelength of 1550 nm taken at room temperature. It is evident that the noise figure (NF) increases as the tapered length increases, which is due to contribution of the whole active region length in spontaneous emission.

For various input signal powers, similar outcomes were found. Additionally, figure (8) illustrates the noise power versus injection current for semiconductor laser amplifier (SLA) at different tapered length. The data in Fig. (8) demonstrate that the output noise power increases rapidly with the increases of the injection current at injection current <60 mA. While the increases in output noise become slight at injection current more than 60 mA. Additionally, when the tapered length increases, the output noise power decreases as well. It is evident that this impact reduces at high drive current values due to higher population inversion and gain.

The output power against input power for semiconductor laser amplifier (SLA) at various tapered length taken at injection current of 120 mA and room temperature is demonstrated in Fig. (9). The output power obviously decreases as the semiconductor laser amplifier (SLA) tapered length increases, this is due to the decrease in the population inversion. Furthermore, the increasing in the input power of semiconductor optical amplifier (SOA) results in saturation of the output power, the reason for this, is that the high input signal leads to maximum depletion of carrier density.

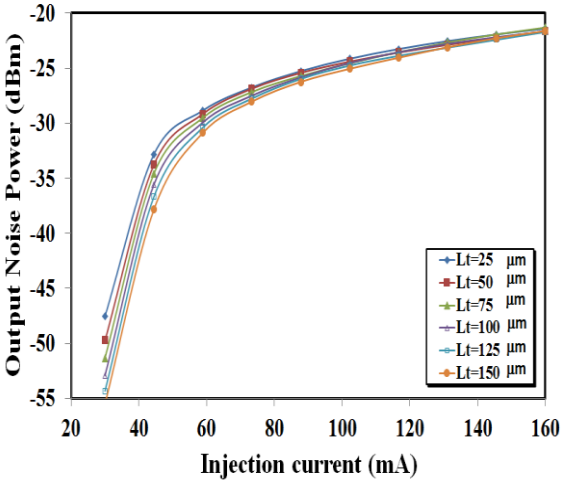

Fig. (8) Output noise power versus injection current at various tapered lengths

4. Conclusions

The influence of tapered active region length (from 25 μm to 150 μm) on the gain dynamics and noise properties of InGaAsP/InP semiconductor laser amplifier (SLA) was studied using a numerical wideband steady-state model. By using this model, it is possible to analysis the wideband performance across a broad range of operating statuses and reveal

the influence of geometrical and material factors on semiconductor laser amplifier (SLA) operation. The results showed that a successful operation of semiconductor laser amplifier (SLA) depends of carful optimization of the values of both tapered length and bias current to obtain a high gain and low noise level. Therefore, the adjustment of the tapered length in semiconductor laser amplifier (SLA) opens the possibility to control device properties, hence improving optimum semiconductor laser amplifier (SLA) device to meet the requirements of specific photonic applications.

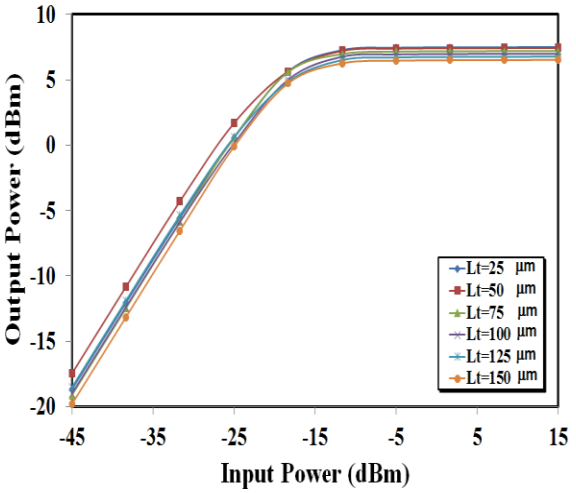

Fig. (9) Output power versus input power at various tapered lengths

References

[1] S. Philippe et al., "Novel design for noise controlled semiconductor optical amplifier", *IEEE Int. Conf. Transp. Opt. Networks* (2009), pp. 1-4.

[2] J. Mork et al., "The Dynamics of Semiconductor Optical Amplifiers: Modeling and Applications", *Opt. Photon. News*, 14(7) (2003) 42-48.

[3] M. Yamada, "Noise in semiconductor optical amplifiers (SOA)", *6th IEEE Int. Conf. Photon. (ICP)*, Kuching, Malaysia (2016) pp. 1-5.

[4] P.P. Baveja et al., "Self-Phase Modulation in Semiconductor Optical Amplifiers: Impact of Amplified Spontaneous Emission", *IEEE J. Quantum Electron.*, 46(9) (2010) 1396-1403.

[5] Y. Said, H. Rezig and A. Bouallegue, "Analysis of noise effects in long semiconductor optical amplifiers", *The Open Opt. J.*, (2008) 61-66.

[6] S. Philippe et al., "Experimental Investigation of Polarization Effects in Semiconductor Optical Amplifiers and Implications for All-Optical Switching", *IEEE J. Lightwave Technol.*, 26(16) (2008) 2977-2985.

[7] S. Philippe et al., "Polarization dependence of non-linear gain compression factor in semiconductor optical amplifier", *Opt. Exp.*, 16(12) (2008) 8641-8648.

[8] H. Ju et al., "SOA-based all-optical switch with subpicosecond full recovery", *Opt. Exp.*, 13(3) (2005) 942-947.

[9] U. Masashin et al., "All optical regeneration using SOA-based polarization discriminated switch injected by transparent assist light", *Proc. SPIE*, 5246 (2003) 263-274.

[10] C. Politi et al., "Dynamic behavior of wavelength converters based on FWM in SOAs", *IEEE J. Quantum Electron.*, 42(2) (2006) 108-125.

[11] F. Wang et al., "All-Optical Clock Recovery Using a Single Fabry–Perot Semiconductor Optical Amplifier", *J. Lightwave Technol.*, 30(11) (2012) 1632-1637.

[12] A . Sharaiha et al., "All-optical logic AND-NOR gate with three inputs based on cross-gain modulation in a semiconductor optical amplifier", *Opt. Commun.*, 265(1) (2006) 322-325.

[13] H. Nakano et al., "10-Gb/s, 4-channel wavelength division multiplexing fiber transmission using semiconductor optical amplifier modules", *J. Lightwave Technol.*, 11(4) (1993) 612-618.

[14] M.J. Connelly, **"Semiconductor Optical Amplifiers"**, Kluwer Academic Pub. (NY, 2004).

[15] R. M. Ibrahim et al., "Temperature-dependency performance of InGaAsP semiconductor laser amplifiers", *Digest J. Nanomater. Biostruct.*, 16(2) (2021) 385-392.

[16] R.M. Ibrahim et al., "Effect of Material Irradiated Type and Spot Size on Spot Center Temperature of a Diode-Pumped Solid State Laser", *Iraqi J. Appl. Phys.*, 20(3) (2024) 540-544.

[17] Y.S. Ong et al., "Characterization of Wideband Semiconductor Optical Amplifiers based on OptiSystem and MATLAB", *The Int. J. Integ. Eng.*, 10(7) (2018).

[18] M.J. Connelly, "Wideband dynamic numerical model of a tapered buried ridge stripe semiconductor optical amplifier gate", *IEE Proc. Circ. Dev. Syst.*, 149(3) (2002).

[19] A. Gahl et al., "Influence of the Confinement Factor on the Wavelength-Dependent Output Properties of a Tapered Traveling-Wave Semiconductor Amplifier", *IEEE Photon. Technol. Lett.*, 11(11) (1999).

[20] M. Fedawy et al., "SOA Output Characteristics: Effect of Amplifier Length and Injected Carrier Density", *Nation. Radio Sci. Conf.*, (2006).

[21] M.J. Connelly, "Wideband semiconductor optical amplifier steady-state numerical model", *IEEE J. Quantum Electron.*, 37(3) (2001) 439-447.

[22] A. Yariv, **"Optical Electronics"**, HWR International (NY, 1985).

[23] D.A. Marcuse, "Computer model of an injection laser amplifier", *IEEE J. Quantum Electron.*, QE-19 (1983) 63-73.
[24] M.J. Connelly, "Wideband dynamic numerical model of a tapered buried ridge stripe semiconductor optical amplifier gate", *IEE Proc. – Circ. Dev. Syst.*, 149(3) (2002) 173-178.
[25] A. Bilenca et al., "Gain and noise properties of InAs/InP quantum dash semiconductor optical amplifiers", *Proc. SPIE*, 6014 (2005) 14-26.
[26] D. Hadass et al., "Gain and Noise Saturation of Wide-Band InAs–InP Quantum Dash Optical Amplifiers: Model and Experiments", *IEEE J. Sel. Topics in Quantum Electron.*, 11(5) (2005)1015-1026.

